



Contents lists available at ScienceDirect

Archives of Biochemistry and Biophysics

journal homepage: www.elsevier.com/locate/yabbi

Original paper

Reaction of *N*-hydroxyguanidine with the ferrous–oxy state of a heme peroxidase cavity mutant: A model for the reactions of nitric oxide synthase [☆]Alycen Pond Nigro, David B. Goodin ^{*}

Department of Molecular Biology, The Scripps Research Institute, 10550 N. Torrey Pines Rd., La Jolla, CA 92037, United States

ARTICLE INFO

Article history:

Received 19 January 2010
and in revised form 19 March 2010
Available online 25 March 2010

Keywords:

Heme enzyme
Protein engineering
Nitric oxide synthase
Metalloenzymes
Cavity complementation
Oxidative catalysis

ABSTRACT

Yeast cytochrome *c* peroxidase was used to construct a model for the reactions catalyzed by the second cycle of nitric oxide synthase. The R48A/W191F mutant introduced a binding site for *N*-hydroxyguanidine near the distal heme face and removed the redox active Trp-191 radical site. Both the R48A and R48A/W191F mutants catalyzed the H₂O₂ dependent conversion of *N*-hydroxyguanidine to *N*-nitrosoguanidine. It is proposed that these reactions proceed by direct one-electron oxidation of NHG by the Fe⁴⁺=O center of either Compound I (Fe⁴⁺=O, porph⁺) or Compound ES (Fe⁴⁺=O, Trp⁺). R48A/W191F formed a Fe²⁺O₂ complex upon photolysis of Fe²⁺CO in the presence of O₂, and *N*-hydroxyguanidine was observed to react with this species to produce products, distinct from *N*-nitrosoguanidine, that gave a positive Griess reaction for nitrate + nitrite, a positive Berthelot reaction for urea, and no evidence for formation of NO[•]. It is proposed that HNO and urea are produced in analogy with reactions of nitric oxide synthase in the pterin-free state.

© 2010 Elsevier Inc. All rights reserved.

Heme enzymes are capable of a diverse range of oxidative reactions defined by the chemistry inherent in the heme cofactor and the way in which substrates are allowed to access reactive intermediates. Examples range from peroxidases, which utilize electron transfer to initiate radical mediated substrate oxidation [1], to the highly energetic oxo-transfer reactions typified by thiolate coordinated heme monooxygenases [2–5]. Many of these reactions are believed to proceed through oxidized heme-centered intermediates similar to the Compound I (Fe⁴⁺=O, porph⁺) state, which has been extensively characterized in heme peroxidases [6–9] but has been more elusive for P450s and nitric oxide synthase (NOS) [10–14]. This is particularly true for NOS, where unfavorable kinetics and high reactivity have precluded the direct observation of the reactive intermediates and their reactions with substrate [15–17]. Thus, many of the mechanistic proposals about NOS been inferential in nature and correspondingly hard won [15,18–20]. It may thus be of interest to make comparisons of the reactions between the well characterized oxidized intermediates of peroxidases and NOS substrate analogs, as this may shed some light on the generality of the NOS catalyzed chemistry or how differences between enzymes define their unique catalytic properties. However, native peroxidases do not bind small molecules in analogy with the arginine and *N*-hydroxyarginine (NHA) substrates of NOS, so their direct reaction with the well characterized heme

intermediates is not possible. Yet, it has been shown that the conserved distal arginine can be removed from cytochrome *c* peroxidase (CcP)¹ to introduce an engineered small molecule binding site by cavity complementation [21], allowing some useful comparisons to be made.

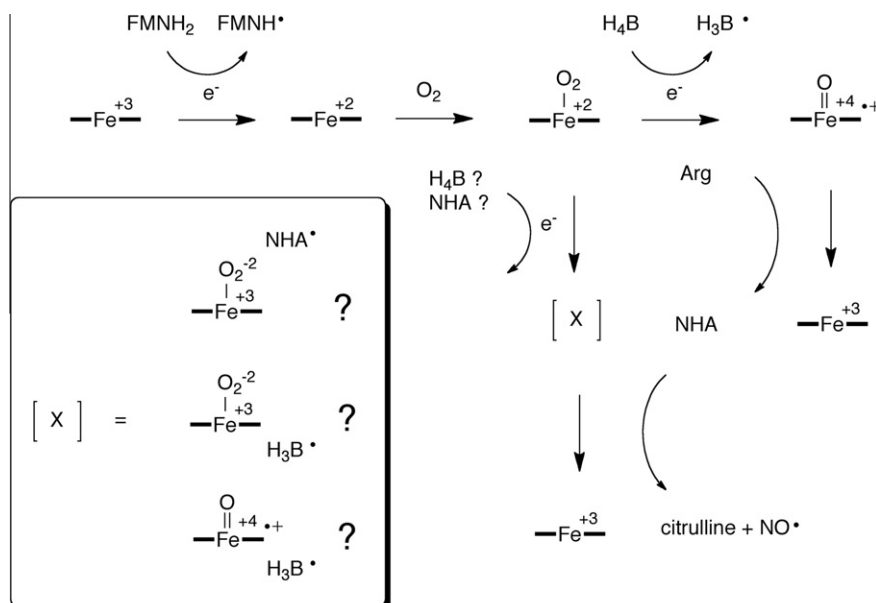
Each of the three main isoforms of mammalian NOS, which contain a tetrahydrobiopterin (H₄B) in addition to the heme at the active site, catalyze the two-cycle oxidation of arginine to produce NO[•] and citrulline [22,23]. In the first cycle, the ferric heme of the arginine-bound enzyme is reduced to the ferrous state by the reductase domain, allowing binding of O₂ (Scheme 1). The Fe²⁺O₂ complex then undergoes a second one-electron reduction from H₄B [24,25] to give a proposed Compound I (Fe⁴⁺=O, porph⁺) intermediate [26], which produces *N*-hydroxyarginine (NHA) in a reaction that is analogous to that catalyzed by cytochrome P450s. In the second enzyme cycle, *N*-hydroxyarginine is further oxidized to give NO[•] and citrulline, but the mechanistic details are less well understood. As with the first cycle, a second electron is provided to reduce the Fe²⁺O₂, and both NHA and H₄B have been proposed to play this role [27]. The chemical nature of the reactive intermediate (labeled X in Scheme 1) for the second cycle is also uncertain,

¹ Abbreviations used: CcP, cytochrome *c* peroxidase; CCP(MKT), cytochrome *c* peroxidase produced by expression in *Escherichia coli* containing Met-Lys-Thr at the N-terminus, Ile at position 53, and Gly at position 152; CN-orn, N⁶-cyanoornithine; NHA, N^ω-hydroxyarginine; NHG, *N*-hydroxyguanidine; NOS, nitric oxide synthase; R48A/W191F, CcP mutant in which Arg-48 is replaced by Ala and Trp-191 is replaced by Phe; WT, wild type CcP; SVD, singular value decomposition; Carboxy-PTIO, 2-(4-carboxyphenyl)-4,4,5,5-tetramethylimidazoline-1-oxyl 3-oxide.

[☆] Funding was provided by the National Institutes of Health Grant GM41049.

^{*} Corresponding author. Fax: +1 (858) 784 2857.

E-mail address: dbg@scripps.edu (D.B. Goodin).



Scheme 1. Reaction cycle of nitric oxide synthase.

but a nucleophilic ferric-peroxy complex coupled to either the NHA• or H₃B• radical has received the most attention (Scheme 1) [16,28,29], while other studies have not excluded a Compound I like intermediate [15]. The ferric-peroxy complex combined with the presence of the radical allows for the three-electron conversion of NHA to NO⁻. In the absence of the additional radical, for example with perin-free NOS [15,27] or in reactions of the ferric enzyme with H₂O₂ [15], the two-electron product HNO or ferrous nitrosyl is observed. However, despite much incisive work and many recent advances, many details of the basic reactions involved in conversion of NHA to products by NOS remain shrouded in uncertainty, and a better understanding of analogous reactions for similar systems might be useful for comparative purposes.

We have previously described a cavity complementation mutant (R48A) of CcP in which Arg-48 is replaced by Ala to generate an artificial cavity that was shown to bind and oxidize *N*-hydroxyguanine (NHG) [21]. CcP is a histidine coordinated heme peroxidase which carries out the H₂O₂ catalyzed oxidation of cytochrome *c* (cyt *c*) [30]. Reaction of the ferric enzyme with H₂O₂ affords a remarkably stable Compound ES which contains Fe⁺⁴=O and a cation radical on nearby Trp-191 [7–9]. Introduction of the R48A cavity allowed binding of NHG at the position of the removed arginine side chain, which is similar to the location of the NHA binding site above the distal heme of NOS. The R48A mutant slowed, but did not abolish the ability of the enzyme to react with H₂O₂ to form Compound ES, and it was found that R48A catalyzed the H₂O₂ dependent oxidation of NHG to a product identified as *N*-nitroso-guanidine. No reaction was observed with WT CcP or with guanidine, and no evidence was observed for production of NO⁻, urea, or cyanamide, the products expected for reactions analogous to the second cycle of NOS. There are important differences between this simple R48A model and NOS which may give rise to the observed alternate reactions. Clearly the identity of the proximal heme ligand may exert significant control over the formation and reactivity of reaction intermediates. In addition, the ability of NOS to resist peroxy bond cleavage while CcP is designed to promote this cleavage may also play a key role. In this regard it is noted that Arg-48 of CcP directly assists peroxy bond cleavage [31], while it has been recently proposed that protonation of the proximal peroxy oxygen atom by bound NHA in NOS may help prevent its cleavage [32]. Thus it may be a key issue to examine

cleaved and un-cleaved ferric peroxy states of model systems for chemical similarity to the reactions of NOS. The Compound ES intermediate formed by reaction of R48A with H₂O₂ contains the ferryl center (Fe⁺⁴=O) and a radical on Trp-191 instead of the more common Compound I (Fe⁺⁴=O, porph⁺) as proposed for P450 and NOS. Finally, a stable Fe⁺²O₂ complex is not accessible in CcP because facile electron donation from Trp-191 causes its rapid reduction and decay through a series of unstable oxidized intermediates [33]. In this work we report on the properties of the R48A/W191F double mutant, which provides an elaborated model for the active site of NOS by providing an NHG-binding site, an accessible Fe⁺²O₂ complex, and a Compound I intermediate that more closely approximates that proposed for NOS. The similarities and differences in reactivity of this mutant is discussed in light of the proposed mechanisms for NHA oxidation in the second reaction cycle of NOS.

Materials and methods

CcP expression and purification

The R48A/W191F mutant of CcP was constructed by site-directed mutagenesis of pT7CCP using the QuikChange site-directed mutagenesis kit (Stratagene) and was over-expressed in *Escherichia coli* BL21 (DE3). The R48A/W191F mutant was purified as described previously [34].

Formation of the ferrous-oxy complex of R48A/W191F CcP

Crystals of the enzyme were dissolved in 0.5 M potassium phosphate buffer at pH 6.0. Enzyme concentration was calculated from the molar extinction of the ferric enzyme at the Soret maximum, as determined by the hemochromogen method [35]. The molar extinction coefficient for the ferric enzyme in 100 mM KPi, pH 6.0, 23 °C is $\epsilon_{409} = 105 \text{ cm}^{-1} \text{ mM}^{-1}$. The method for creating the Fe⁺²O₂ complex was based on that of Miller et al. [36] with minor alterations. Briefly, a solution of ferric protein (5–20 μM) was prepared in 100 mM KPi buffer, pH 6.0 in a 1 cm path-length sealed quartz cuvette. The sample was converted to the Fe⁺²CO complex by reduction with 1.5 equivalents of dithionite from a calibrated

stock solution under a CO atmosphere, and formation of the Fe⁺²CO ferrous complex was monitored by absorption at 420 nm. CO was then exchanged for O₂ by bubbling in the dark for 5 min, followed by CO photolysis by a water-filtered 75 W Xe light source for 10 s. Formation of Fe⁺²O₂ was monitored a blue shift of the Soret band back to 416 nm.

Spectrometry and kinetic measurements

UV-visible absorption spectra were collected at 23 °C using a Hewlett–Packard 8435 diode array spectrometer. For binding titrations, a solution of approximately 5 μM protein was equilibrated in 100 mM KPi buffer at pH 6.0 for 30 min. Spectra were then recorded at equilibrium, following the addition of small aliquots of ligand also corrected to pH 6.0. Dissociation constants and cooperativity were determined using Scatchard and Hill plots. Kinetic spectrometric measurements were conducted using the kinetics module of the Hewlett–Packard 8435 diode array spectrometer, or an OLIS RSM1000 rapid-scan stopped flow instrument. Fits to kinetic data were performed using SpecFit.

NO analysis

Following reaction of the Fe⁺²O₂ or Compound I states of R48A/W191F with ligand, two methods were used for detection of nitrogen oxides. First, the Griess reaction was used as previously described to analyze for total nitrate and nitrite, the breakdown products of NO under aerobic conditions [21]. Nitrate was first converted to nitrite using nitrate reductase and NADH for 20 min at 37 °C before performing the Griess assay, and reaction was measured by absorbance at 540 nm. The linearity of response was established by using standard solutions.

Analysis for NO was also performed using the NO scavenger 2-(4-carboxyphenyl)-4,4,5,5-tetramethylimidazole-1-oxyl 3-oxide (carboxy-PTIO) [37,38]. Conversion of carboxy-PTIO, a nitronyl nitroxide to the imino nitroxide by NO was monitored by room temperature EPR. Carboxy-PTIO was purchased from Alexis Biochemical Corporation and used without further purification. The ferrous–oxy complex of 20 μM R48A/W191F CcP was prepared in the presence or absence of 500 μM NHG as described above. Carboxy-PTIO was added to the reaction cuvette after bubbling the solution with O₂ and prior to photolysis to prevent reaction with residual dithionite. Control conversion of PTIO to the imino nitroxide was performed by addition of known aliquots of NO solution. EPR spectra were recorded on a Bruker EMX X-band spectrometer using a TE102 rectangular cavity at room temperature, using a 19 bore quartz micro-capillary sample cell. EPR spectra were acquired at a frequency of 9.68 GHz and 10 mW microwave power, 1.0 G modulation amplitude at 100 kHz.

Urea analysis

The Berthelot reaction [39] was used to analyze reactions containing R48A/W191F Fe⁺²O₂, produced by photolysis of Fe⁺²CO in the presence of O₂, and NHG for formation of urea. In this case, an excess of enzyme (10 μM NHG, 20 μM enzyme) was used to cause complete conversion of NHG to products. Formation of the Fe⁺²O₂ complex in 100 mM KPi pH 7 was verified by monitoring UV/vis during photolysis and the incubations with NHG were allowed to proceed for 360 s before analysis for urea. Protein was removed from the samples by ultra-filtration, and 5 U urease were added before incubation at 50 °C for 30 min. To a 1 ml aliquot of the resulting solution was added 100 μl of a solution containing 0.74 M phenol and 1 mM sodium nitroprusside, and 200 μl of a solution containing 0.37 M NaOH, 0.4 M Na₂HPO₄ and 1% NaOCl. After incubation for a further 30 min at 50 °C, formation of indophenol was measured at 636 nm and urea concentrations deter-

mined from standard curves containing known amounts of urea and/or NH₄.

Results

R48A/W191F properties and ligand binding

The R48A/W191F double mutant (Fig. 1) was constructed to combine the NHG-binding cavity of R48A with a variant of the enzyme capable of forming alternate oxidized intermediates in order to explore potential differences in reactivity. Titration of R48A/W191F CcP with NHA, guanidine or arginine resulted in only small, non-saturating optical changes indicating a lack of interaction between the ligand and the cavity. However, addition of NHG resulted in a dramatic perturbation of the heme optical spectrum as shown in Fig. 2. Clear isosbestic points were observed at 340, 412, 475, 530, and 605 nm indicating a two-state conversion associated with a red shift of the Soret band from 409 to 415 nm coupled with a decrease in intensity of the charge transfer bands at 508 and 640 nm and the appearance of α/β bands at 541 and 570 nm. These changes are consistent with the NHG induced conversion from high- to low-spin as was observed for the R48A single mutant upon binding of NHG [21]. The spin-state change is consistent with conversion from 5- to 6-coordinate heme, suggesting that NHG binds directly to the ferric iron, as was observed for the R48A single mutant. Fits to the titration data of Fig. 2 showed that NHG binds to R48A/W191F with somewhat higher affinity ($K_d = 3.37$ mM) than to R48A ($K_d = 8.48$ mM).

NHG oxidation by the peroxide shunt pathway

R48A/W191F was observed to react with H₂O₂ to give a transient Compound I species which was capable of oxidizing NHG but not guanidine. As shown in Fig. 3, reaction of R48A/W191F with H₂O₂ in the absence of NHG produced a rapid bleaching of the Soret absorbance at 408 nm followed by a slower partial recovery. SVD analysis of 1 ms spectral scans using a sequential A > B > C model gave component spectra with Soret absorbance maxima at 408, 408 (bleached), and 414 nm, consistent with species contain-

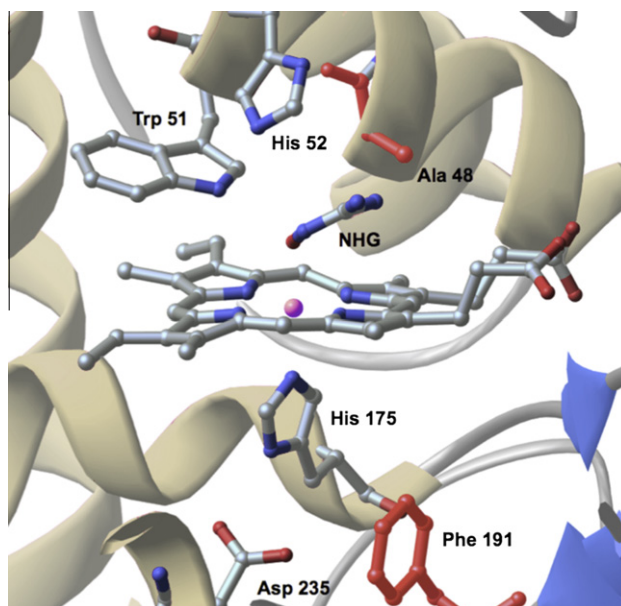


Fig. 1. Active site model for the NHG-binding variant R48A/W191F of CcP based on the structure of the NHG bound state of R48A (pdb code 1DJ5).

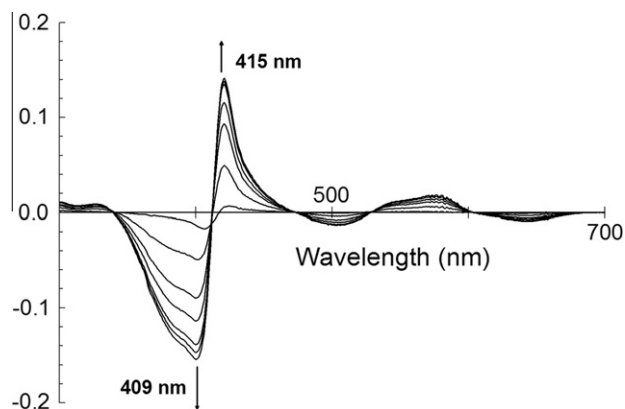


Fig. 2. Binding of NHG to the R48A/W191F CcP mutant. Optical difference spectra for R48A/W191F (5 μ M) in 100 mM KPi pH 6.0, 2 ml volume upon successive additions of 5 μ l of 500 mM NHG (corrected to pH 6.0).

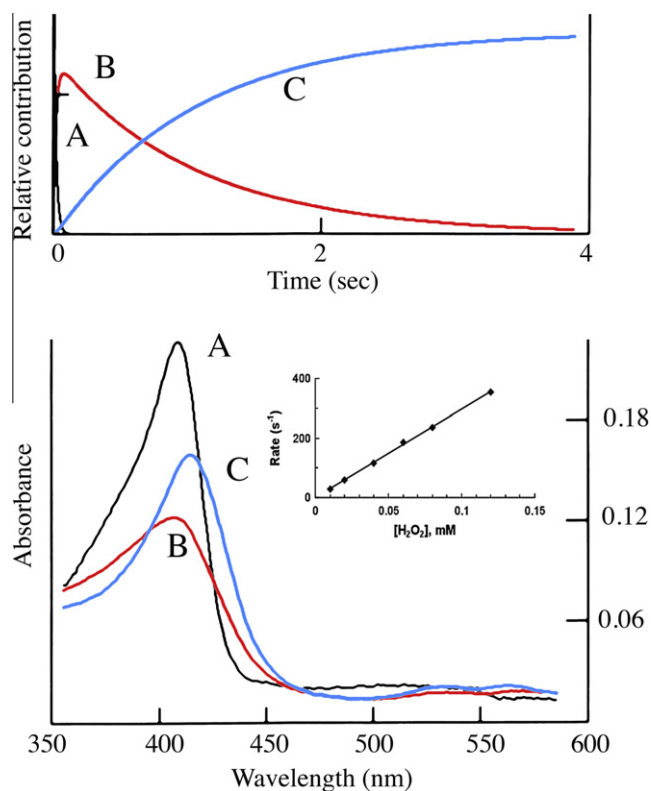


Fig. 3. Formation and decay of Compound I following reaction of R48A/W191F CcP with H_2O_2 by rapid-scan stopped flow mixing of 5 μ M protein against 20 μ M H_2O_2 in 100 mM KPi pH6, 25 $^\circ\text{C}$. Data analysis by single value decomposition using a model for sequential conversion of three species, A, B and C, produced the spectra and time courses shown in the lower and upper panels, respectively, and represent the ferric, Compound I and Compound II states. Pseudo-first order rate constants for the formation of Compound I are plotted as a function of H_2O_2 (inset) to give a bimolecular rate of $2.96 \times 10^6 \text{ M}^{-1} \text{ s}^{-1}$.

ing high-spin ferric heme (A), Compound I ($\text{Fe}^{4+}=\text{O}$, porph $^{+}$) (B), and Compound II ($\text{Fe}^{4+}=\text{O}$) (C), respectively. The H_2O_2 dependent bimolecular rate constant for R48A/W191F Compound I formation ($k_1 = 3.0(6) \times 10^6 \text{ M}^{-1} \text{ s}^{-1}$) was about 3-fold higher than that observed previously for R48A Compound ES formation ($k_1 = 1.33 \times 10^6 \text{ M}^{-1} \text{ s}^{-1}$) [21]. In the absence of NHG, formation of Compound I was followed by a slower H_2O_2 independent conversion to Compound II with a rate of $0.95(6) \text{ s}^{-1}$ which was then stable for many minutes. However, the presence of NHG, but not guanidine,

caused a marked acceleration in the rate of recovery in the absorbance at 408 nm which may result from the reaction of NHG with either the Compound I or Compound II species. As shown in Fig. 4, the rate of return to the ferric state was dependent on NHG concentration, giving a bimolecular rate constant of $1.7(4) \times 10^5 \text{ M}^{-1} \text{ s}^{-1}$. NHG did not cause a corresponding increase in the rate of decay of Compound ES for WT CcP, indicating that this reaction was specific for NHG-binding within the R48A cavity. The reaction of R48A/W191F Compound I with NHG afforded a yellow product. After allowing solutions containing 5 μ M R48A/W191F, 1 mM NHG and 1 mM H_2O_2 in 50 mM KPi, pH 6 to react at 25 $^\circ\text{C}$ for 10 min, the enzyme was removed by ultra-filtration and the solution gave absorption spectra (Fig. 5) with maxima at 260 and 400 nm, essentially identical to spectra for the products of analogous reactions of the R48A single mutant with NHG and H_2O_2 . This product was previously identified as *N*-nitrosoguanidine, and these results thus suggest that the same species is produced by both R48A and R48A/W191F in reactions of NHG with H_2O_2 .

NHG oxidation via the Fe^{2+}O_2 complex

Formation of the Fe^{2+}O_2 state for R48A/W191F in the absence of NHG was achieved by photolysis of the Fe^{2+}CO complex (absorption maxima at 423, 542, and 570 nm) in the presence of O_2 saturated buffer (Fig. 6A). Immediately following photolysis, the Fe^{2+}CO complex was converted to a species with peaks at 416, 545 and 580 nm which decayed slowly back to the ferric state over a period of approximately 1 h at room temperature. Multiple isosbestic points in the visible and Soret region during this conversion indicate that no significant accumulation of intermediates occurred during the reaction. Assignment of this species to the Fe^{2+}O_2 complex was based on the similarity of its optical spectrum to those of the analogous species for the W191F single mutant [36] and horseradish peroxidase (HRP) [40]. The rate of auto-oxidation of the Fe^{2+}O_2 complex was found to be $9.4 \times 10^{-4} \text{ s}^{-1}$ at 25 $^\circ\text{C}$. No evidence for the formation of a stable Fe^{2+}O_2 complex was observed for either the R48A single mutant or WT CcP, which instead form Compound ES following the rapid reduction of Fe^{2+}O_2 by Trp-191 [36]. Formation of the R48A/W191F Fe^{2+}CO and Fe^{2+}O_2 complexes were also observed in the presence of NHG. However, the decay of Fe^{2+}O_2 to the ferric state was accelerated by NHG in a concentra-

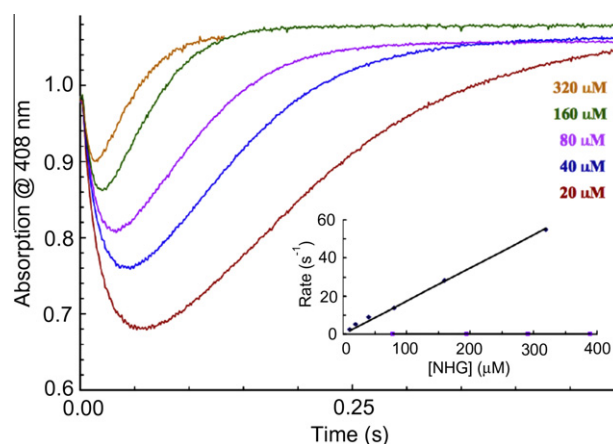


Fig. 4. Effect of NHG on the decay of R48A/W191F Compound I. Compound I was formed as described in Fig. 3 in the presence of 20 (red), 40 (blue), 80 (magenta), 160 (green) and 320 (orange) μ M NHG. Shown in the inset are the substrate dependent rates for conversion of Compound I to Compound II for R48A/W191F (blue) and WT CcP (magenta) to give bimolecular rate constants of 1.73×10^5 and $2.8 \times 10^1 \text{ M}^{-1} \text{ s}^{-1}$, respectively. (For interpretation of color mentioned in this figure the reader is referred to the web version of the article.)

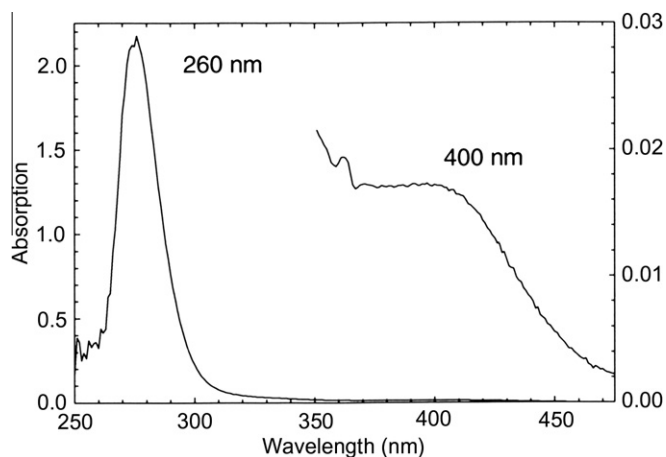


Fig. 5. UV/vis absorption spectrum of the product following reaction of 5 μM R48A/W191F with 1 mM H_2O_2 in the presence of 1 mM NHG. After incubation at 25 $^\circ\text{C}$ for 30 min the protein was removed by ultra-filtration before recording the spectrum.

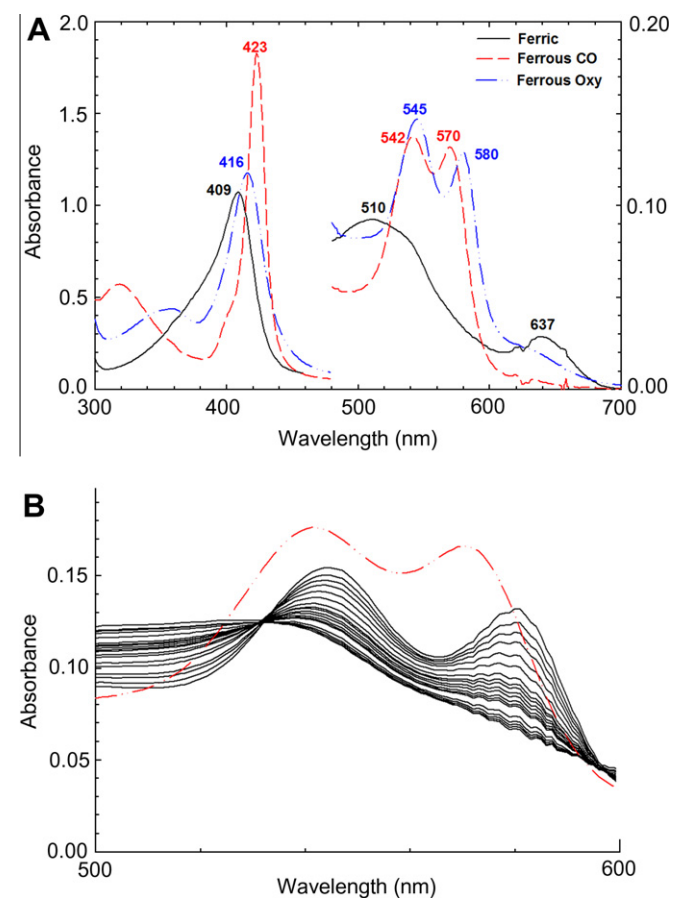


Fig. 6. Formation and decay of the Fe^{2+}O_2 complex of R48A/W191F. (A) UV/vis spectra of 10 μM R48A/W191F in 100 mM KPi pH 6.0 in the Fe^{3+} (solid black), Fe^{2+}CO (red dash) and Fe^{2+}O_2 (blue dot dash) formed after photolysis of the Fe^{2+}CO complex in the presence of O_2 . (B) Visible absorption region showing the conversion of the Fe^{2+}CO complex (red dash) to Fe^{2+}O_2 upon photolysis and its subsequent decay back to the resting Fe^{3+} state over approximately 1 h (black). (For interpretation of color mentioned in this figure the reader is referred to the web version of the article.)

tion-dependent manner, suggesting a reaction between NHG and the Fe^{2+}O_2 complex. As shown in Fig. 7, the reaction of NHG with the Fe^{2+}O_2 state was exponential and dependent on NHG concentration, giving a bimolecular rate constant of $29.2 \text{ M}^{-1} \text{ s}^{-1}$, while

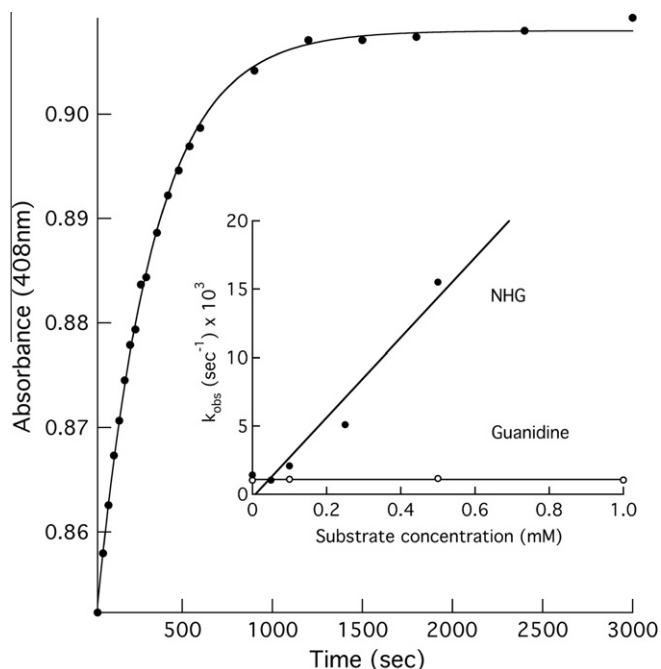


Fig. 7. Kinetics for the reaction of NHG with the Fe^{2+}O_2 complex of R48A/W191F. Absorbance at 408 nm representing the recovery of the Fe^{3+} state following photolysis of the Fe^{2+}CO complex in the presence of O_2 and 50 μM NHG. Fit to a single exponential (solid curve) gave k_{obs} which is shown as a function of NHG and guanidine concentration (inset) to give the bimolecular rate constants reported in the text.

the presence of guanidine had no observable effect on the slow auto-oxidation rate. Analogous reactions showed that NHG did not react with the Fe^{2+}O_2 complex of the W191F single mutant. For example, the absorbance ($A_{408} = 0.453$) immediately after formation of the Fe^{2+}O_2 complex did not change significantly ($A_{408} = 0.457$) after 60 s reaction with 200 μM NHG.

In the presence of the R48A/W191F Fe^{2+}O_2 complex, NHG was converted to nitrogen oxide product(s) distinct from that produced in reactions with H_2O_2 . Unlike the case for the reaction with H_2O_2 , no yellow product was observed following ultra-filtration to remove protein, suggesting that *N*-nitrosoguanidine is not formed in the reaction with R48A/W191F Fe^{2+}O_2 . In addition, nitrogen oxides were detected in samples following the reaction of R48A/W191F Fe^{2+}O_2 with NHG. Analysis for total nitrite + nitrate, the aerobic breakdown products of NO^\cdot and HNO , was performed using nitrate reductase and the Griess reaction [21]. As shown in Fig. 8, reactions of NHG with the R48A/W191F Fe^{2+}O_2 complex produced significantly higher levels of nitrite + nitrate relative to control reactions of WT or W191F. In addition, this positive Griess reaction was dependent on the presence of both NHG and the Fe^{2+}O_2 state. Together, these results show that NHG in the presence of the Fe^{2+}O_2 state of R48A/W191F, binds to the R48A cavity and reacts to give products that give a positive Griess reaction. Further analysis suggests that HNO and urea may be produced in the reaction of the R48A/W191F Fe^{2+}O_2 complex with NHG. The positive Griess reaction without production of *N*-nitrosoguanidine, suggested that the reaction may initially produce either NO^\cdot or HNO . However, several methods failed to detect the formation of NO^\cdot in these reactions. UV/vis spectra of the enzyme following reaction showed final return to the ferric state, without evidence for formation of the Fe^{3+}NO or Fe^{2+}NO complexes. Attempts to detect NO^\cdot using an NO -specific electrode during photolysis of R48A/W191F Fe^{2+}CO in the presence of O_2 and NHG were also unsuccessful. Finally, the nitric oxide scavenger carboxy-PTIO was used to analyze reactions for transient NO^\cdot production. Carboxy-PTIO is a nitronyl nitroxide

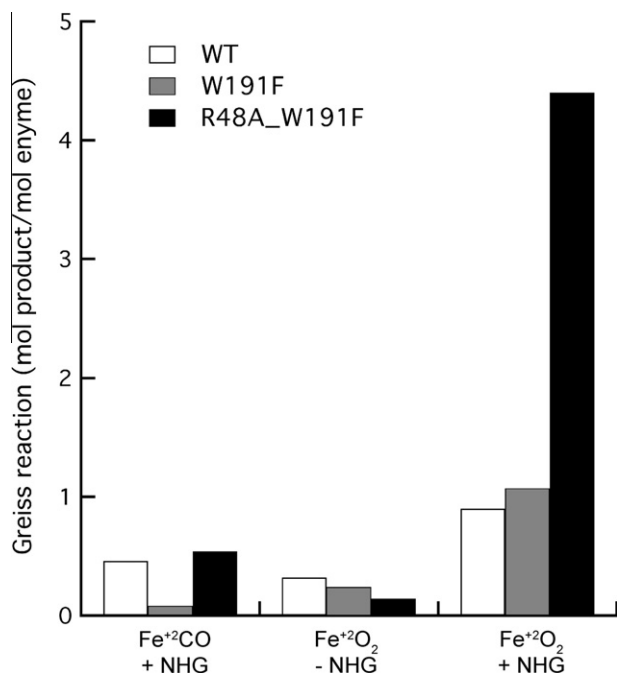


Fig. 8. Analysis for total nitrate and nitrite formed in reactions of WT, W191F, and R48A/W191F with NHG. Samples of enzyme (5 μ M) were converted to the Fe²⁺O₂ or Fe²⁺CO complexes as described in Methods and Fig. 6 and incubated in the presence or absence of 200 μ M NHG for 30 min before removal of protein by ultra-filtration and analysis of the filtrate for total nitrate and nitrite using nitrate reductase and the Griess reaction. Total product measured by this assay was normalized using a standard curve for nitrate.

which reacts rapidly with NO[•] to form the corresponding imino nitroxide [37,38]. Both of these compounds give distinct electron paramagnetic resonance (EPR) signals, allowing detection of transiently formed NO[•]. However, as shown in Fig. 9, photolysis of the R48A/W191F Fe²⁺CO complex in the presence of O₂, NHG and carboxy-PTIO failed to give evidence for the conversion of the nitronyl nitroxide to the imino nitroxide, while addition of NO[•] to the reactions produced the expected change in EPR signal. Taken

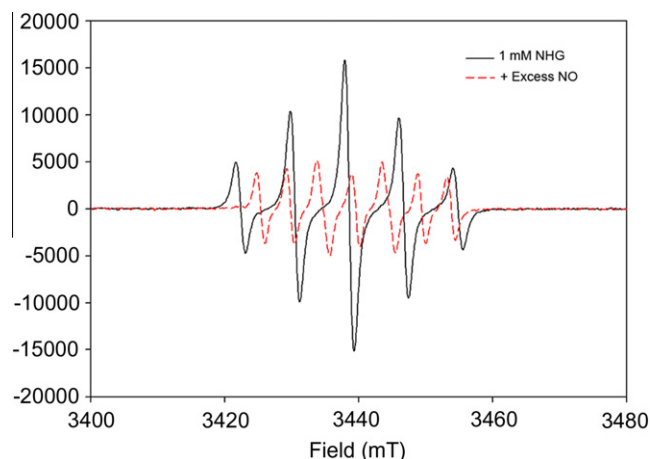


Fig. 9. EPR analysis for NO[•] formation during reaction of Fe²⁺O₂ complex of R48A/W191F with NHG. A reaction mixture containing 20 μ M R48A/W191F and 500 μ M NHG and 10 μ M PTIO was prepared in the Fe²⁺O₂ state allowed to react for 20 min before recording the RT EPR spectrum at room temperature. The signal (black) shows only the 5 hyperfine transitions corresponding to the un-reacted PTIO nitronyl nitroxide and no evidence for the imino nitroxide (red) which was produced by subsequent addition of excess NO to the solution. (For interpretation of color mentioned in this figure the reader is referred to the web version of the article.)

together these results suggest that HNO may be the species responsible for the positive Griess reaction, given that neither NO[•] nor *N*-nitrosoguanidine is observed. Finally, analysis of reaction mixtures suggested formation of urea in the reaction of R48A/W191F Fe²⁺O₂ complex with NHG. Urea would be the expected product if the reaction was analogous to the NOS catalyzed oxidation of NHA to form either NO[•] or HNO and citrulline [16]. Following reaction of 20 μ M R48A/W191F Fe²⁺O₂ with 10 μ M NHG, analysis using urease and the Berthelot [39] reaction gave 7.8 μ M urea in the sample. Cyanamide, the analog of cyanornithine, which has also been observed in reactions of NOS driven by the peroxide shunt, was not observed to give a positive Berthelot reaction, suggesting that the analysis is specific for urea and not cyanamide.

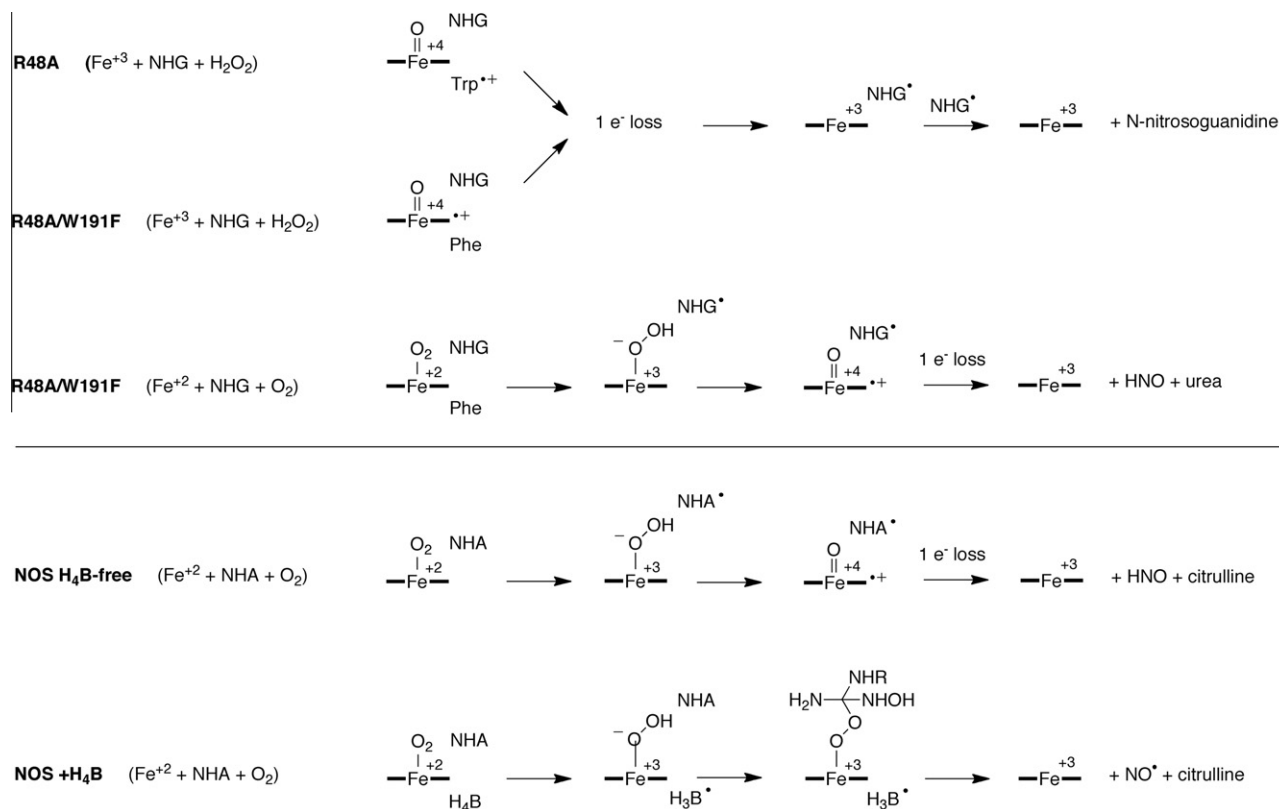
Discussion

The reactions carried out by the second cycle of NOS in which NHA is converted to NO[•] and citrulline are the least well understood aspects of this important enzyme. This is due in part to the instability of the proposed oxidized intermediates, and in consequence, their identity and reactions have been difficult to study directly. While there are many important differences between the active site of NOS and classic peroxidases, including the identity of the axial heme ligand, it would nevertheless be of interest to examine the reactivity of the well characterized intermediates of a peroxidase with NOS substrate analogs. While this is not possible with wild-type peroxidases due to their inability to bind substrates in a position analogous to NOS, engineered binding sites provide an approach for this.

Reactions of R48A/W191F with hydroxyguanidine

Several interesting comparisons can be made between the reactions of R48A/W191F CcP and those of the second reaction cycle of NOS. Like the R48A single mutant, R48A/W191F retains the capacity to bind NHG, but not guanidine due to cavity complementation as a result of the removal of the Arg-48 side chain [21]. In addition, replacement of the Trp-191 radical site with phenylalanine prevents participation of the Trp-191 radical in this engineered NHG-binding cavity mutant. This changes the nature of the oxidized intermediate formed upon reaction of the ferric enzyme with H₂O₂. Thus, rather than forming a Compound ES like state (Fe⁴⁺=O Trp^{•+}) as observed for WT CcP and R48A, the R48A/W191F mutant is observed to give an intermediate similar to Compound I (Fe⁴⁺=O, porph^{•+}) as seen in HRP, and proposed for P450 and in the first reaction cycle of NOS. In addition, removal of the redox active Trp-191 allows observation of the Fe²⁺O₂ state, which is not accessible in WT CcP [36]. These two properties give rise to a novel opportunity to examine the reactions of oxidized states of the heme with a hydroxyguanidine compound bound in the distal heme cavity, a context that is similar to that for the reactions of the second reaction cycle of NOS.

A proposal for the reactions observed between NHG and R48A/W191F that is consistent with the results of this work is presented in Scheme 2. R48A and R48A/W191F react with H₂O₂ to produce analogs of Compound ES and Compound I, respectively, as has been well characterized for WT CcP and W191F. These species have the potential to produce a two-electron oxidation of substrate, but vary in the location of the radical species coupled to the Fe⁴⁺=O center. Both of these species react with NHG to produce the same product, previously shown to be *N*-nitrosoguanidine [21]. This reaction only proceeds in the context of the R48A mutation, suggesting that it is the result of the localization of NHG within in the distal R48A cavity, as shown by X-ray crystallography. It was



Scheme 2. Proposed reactions of CcP cavity mutants with *N*-hydroxyguanidine.

proposed that each reaction with H_2O_2 oxidizes NHG by one-electron to produce a radical, two of which subsequently disproportionate to give *N*-nitrosoguanidine [21]. In the current work, the observation of the same product for both the Compound ES (R48A) and Compound I (R48A/W191F) analogs of this reaction suggests that it is the $\text{Fe}^{4+}=\text{O}$ center and not the position or identity of the racial species that is responsible for this reaction. This supports the notion that the $\text{Fe}^{4+}=\text{O}$ center itself catalyzes the one-electron oxidation of NHG bound in the R48A cavity, and additionally suggests that the other oxidation equivalent held in Compound I or Compound ES is lost to an unknown location in each of these reactions (Scheme 2).

The R48A/W191F double mutant also allows accumulation of the Fe^{2+}O_2 state, which reacts with NHG to produce products that suggest some similarity with reactions of NOS in the pterin-free form, or when driven by the peroxide shunt [27,29]. NHG accelerates the decay of the Fe^{2+}O_2 state to form product(s) which give a positive Griess reaction. However, no evidence was seen for formation of NO^\bullet or *N*-nitrosoguanidine (which also produces a positive Griess reaction), suggesting the possible formation of HNO. Evidence for the formation of urea was also observed in this reaction, which would be the product analogous to the NOS catalyzed conversion of NHA to citrulline [16]. The reaction only proceeds for R48A/W191F and not W191F, suggesting that it requires the R48A binding cavity above the distal heme plane. The reaction with the Fe^{2+}O_2 state has the potential to produce a three-electron oxidation of substrate, but the proposed formation HNO and urea suggests that only two oxidation equivalents are used in the reaction. One possibility for this could result from a slow, one-electron leakage into the Fe^{2+}O_2 state from an alternative reducing agent, such as a distant tyrosine residue before reaction with NHG. This would produce a species equivalent to the ferric-peroxy complex, and in the context of the of CcP active site this complex would most likely decay rapidly by heterolytic peroxy bond cleavage to form

Compound I. However, this would then be expected to react with NHG to give the same products as seen in the reaction of ferric enzyme with peroxide, and this is at variance with our observations. In addition, slow electron leakage into the Fe^{2+}O_2 state before reaction with NHG would not explain the NHG dependent acceleration of the Fe^{2+}O_2 decay. Thus, we propose that our data are most consistent with the model proposed in Scheme 2 in which NHG itself is the electron donor to the Fe^{2+}O_2 state to form an NHG radical and an enzyme intermediate equivalent to the ferric-peroxy complex. It is possible that this is followed by nucleophilic attack of the ferric-peroxy complex on NHG^\bullet as has been proposed for NOS [15,16,20,28,41], but it is considered more likely that in the context of the CcP active site, the ferric-peroxy state would rapidly form Compound I. One-electron oxidation of the NHG^\bullet radical by the $\text{Fe}^{4+}=\text{O}$ center of Compound I with loss of the second equivalent as proposed above for the reaction with peroxide could produce the proposed products HNO and urea in an overall two-electron oxidation of NHG. The fact that no intermediates are observed in the conversion of the Fe^{2+}O_2 state to the resting enzyme would be consistent with electron donation from NHG as the rate limiting step.

Relevance to reactions of NOS

As indicated in Scheme 1, several proposals have been made about the reactive species responsible for the three-electron conversion of NHA to NO^\bullet and citrulline. These primarily differ in the source of the second electron used for reduction of the Fe^{2+}O_2 state. Early studies proposed NHA as the source of this second electron, while more recent studies have favored electron donation from the pterin [16,27–29,32]. In addition it has not been clear whether the reactive species (X in Scheme 1) corresponds to a Compound I like state or an un-cleaved ferric hydroperoxy intermediate [15]. Current proposals favor the later which is believed to make a cova-

lent adduct with NHA by nucleophilic attack of the distal peroxy oxygen atom (Scheme 2). It is of note that reaction of pterin-free NOS, or ferric NOS with H₂O₂ produce the alternate products HNO or heme-bound nitrosyl (Fe⁺²NO) and a mixture of citrulline and cyanoornithine, suggesting that participation of the H₃B[•] radical may play a role in controlling whether NO[•] or HNO is produced [27,41–43]. It is possible that the reactions of pterin-free NOS forms these alternate products in reactions that are analogous to those we have described for the R48A/W191F Fe⁺²O₂ state. Specifically, if pterin is not present to provide the second electron to the Fe⁺²O₂ state, then NHA becomes an alternate source of this second electron, and this leads to formation of Compound I and an NHA[•] radical (Scheme 2). Subsequent one-electron oxidation of this radical by the Fe⁺⁴=O species with the loss of a second equivalent would give the alternate product HNO. Thus, while the reactions of the peroxidase based cavity mutants described here do not provide a completely analogous model for the structure and function of NOS, the similarities and differences observed may provide useful comparisons for the reactions catalyzed by NOS under unusual conditions, and these comparisons may help to define the important features of these reactions.

Acknowledgments

The authors thank Dr. Anna-Maria Hays Putnam, and Prof. Stefan Vetter for valuable discussions.

References

- [1] C. Obinger, Arch. Biochem. Biophys. (this issue).
- [2] P.R. Ortiz de Montellano, Cytochrome P450: Structure, Function, and Biochemistry, Plenum, New York, 1995.
- [3] E.J. Mueller, P.J. Loida, S.G. Sligar, in: P.R. Ortiz de Montellano (Ed.), Cytochrome P450: Structure, Mechanism and Biochemistry, Plenum, New York, 1995, pp. 83–124.
- [4] J.H. Dawson, Science 240 (1988) 433–439.
- [5] M. Sono, M.P. Roach, E.D. Coulter, J.H. Dawson, Chem. Rev. 96 (1996) 2841–2887.
- [6] D. Dolphin, A. Forman, D.C. Borg, J. Fajer, R.H. Felton, Proc. Natl. Acad. Sci. USA 68 (1971) 614–618.
- [7] M. Sivaraja, D.B. Goodin, M. Smith, B.M. Hoffman, Science 245 (1989) 738–740.
- [8] J.E. Huyett, P.E. Doan, R. Gurbiel, A.L.P. Houseman, M. Sivaraja, D.B. Goodin, B.M. Hoffman, J. Am. Chem. Soc. 117 (1995) 9033–9041.
- [9] A.L.P. Houseman, P.E. Doan, D.B. Goodin, B.M. Hoffman, Biochemistry 32 (1993) 4430–4443.
- [10] R. Davydov, T.M. Makris, V. Kofman, D.E. Werst, S.G. Sligar, B.M. Hoffman, J. Am. Chem. Soc. 123 (2001) 1403–1415.
- [11] X. Sheng, J.H. Horner, M. Newcomb, J. Am. Chem. Soc. (2008).
- [12] M. Newcomb, J.A. Halgrimson, J.H. Horner, E.C. Wasinger, L.X. Chen, S.G. Sligar, Proc. Natl. Acad. Sci. USA (2008) 8179–8184.
- [13] M. Newcomb, R. Zhang, R.E. Chandrasena, J.A. Halgrimson, J.H. Horner, T.M. Makris, S.G. Sligar, J. Am. Chem. Soc. (2006) 4580–4581.
- [14] T. Egawa, H. Shimada, Y. Ishimura, Biochem. Biophys. Res. Commun. (1994) 1464–1469.
- [15] J. Woodward, M.M. Chang, N.I. Martin, M.A. Marletta, J. Am. Chem. Soc. 131 (2009) 297–305.
- [16] M.A. Marletta, J. Biol. Chem. 268 (1993) 12231–12234.
- [17] J. Tejero, A. Biswas, Z.-Q. Wang, R.C. Page, M.M. Haque, C. Hemann, J.L. Zweier, S. Misra, D.J. Stuehr, J. Biol. Chem. 283 (2008) 33498.
- [18] C.-C. Wei, Z.-Q. Wang, J. Tejero, Y.P. Yang, C. Hemann, R. Hille, D.J. Stuehr, J. Biol. Chem. 283 (2008) 11734–11742.
- [19] H. Huang, J.M. Hah, R.B. Silverman, J. Am. Chem. Soc. 123 (2001) 2674–2676.
- [20] J.T. Groves, C.C. Wang, Curr. Opin. Chem. Biol. 4 (2000) 687–695.
- [21] J. Hirst, D.B. Goodin, J. Biol. Chem. 275 (2000) 8582–8591.
- [22] B.R. Crane, A.S. Arvai, D.K. Ghosh, C. Wu, E.D. Getzoff, D.J. Stuehr, J.A. Tainer, Science 279 (1998) 2121–2126.
- [23] C.S. Raman, H. Li, P. Martásek, V. Král, B.S. Masters, T.L. Poulos, Cell 95 (1998) 939–950.
- [24] A.R. Hurshman, C. Krebs, D.E. Edmondson, B.H. Huynh, M.A. Marletta, Biochemistry 38 (1999) 15689–15696.
- [25] C.-C. Wei, Z.-Q. Wang, Q. Wang, A.L. Meade, C. Hemann, R. Hille, D.J. Stuehr, J. Biol. Chem. (2001) 315–319.
- [26] R. Davydov, A.P. Ledbetter, P. Martásek, M. Larkhin, M. Sono, J.H. Dawson, B.S.S. Masters, B.M. Hoffman, Biochemistry 41 (2002) 10375–10381.
- [27] A.R. Hurshman, M.A. Marletta, Biochemistry 41 (2002) 3439–3456.
- [28] H.G. Korth, R. Sustmann, C. Thater, A.R. Butler, K.U. Ingold, J. Biol. Chem. 269 (1994) 17776–17779.
- [29] S. Adak, Q. Wang, D.J. Stuehr, J. Biol. Chem. 275 (2000) 33554–33561.
- [30] T.L. Poulos, J. Kraut, J. Biol. Chem. 255 (1980) 8199–8205.
- [31] L.B. Vitello, J.E. Erman, M.A. Miller, J. Wang, J. Kraut, Biochemistry 32 (1993) 9807–9818.
- [32] T. Doukov, H. Li, M. Soltis, T.L. Poulos, Biochemistry (2009).
- [33] M.A. Miller, D. Bandyopadhyay, J.M. Mauro, T.G. Traylor, Kraut, Biochemistry 31 (1992) 2789–2797.
- [34] M.M. Fitzgerald, M.J. Churchill, D.E. McRee, D.B. Goodin, Biochemistry 33 (1994) 3807–3818.
- [35] K.G. Paul, H. Theorell, A. Akesson, Acta Chem. Scand. 7 (1953) 1284–1287.
- [36] M.A. Miller, D. Bandyopadhyay, J.M. Mauro, T.G. Traylor, J. Kraut, Biochemistry 31 (1992) 2789–2797.
- [37] T. Akaïke, H. Maeda, Methods Enzymol. 268 (1996) 211–221.
- [38] T. Akaïke, M. Yoshida, Y. Miyamoto, K. Sato, M. Kohno, K. Sasamoto, K. Miyazaki, S. Ueda, H. Maeda, Biochemistry 32 (1993) 827–832.
- [39] L. Kersher, J. Ziegenhorn, in: H.U. Bergmeyer (Ed.), Methods Enzym. Anal., Weinheim, VCH, 1985, pp. 444–453.
- [40] V.F. Ximenes, L.H. Catalani, A. Campa, Biochem. Biophys. Res. Commun. 287 (2001) 130–134.
- [41] D.J. Stuehr, C.-C. Wei, Z. Wang, R. Hille, Dalton Trans. (Cambridge, England: 2003) (2005) 3427–3435.
- [42] S. Donzelli, M.G. Espey, W. Flores-Santana, C.H. Switzer, G.C. Yeh, J. Huang, D.J. Stuehr, S.B. King, K.M. Miranda, D.A. Wink, Free Radical Biol. Med. 45 (2008) 578–584.
- [43] C.-C. Wei, Z.-Q. Wang, C. Hemann, R. Hille, D.J. Stuehr, J. Biol. Chem. 278 (2003) 46668–46673.